Applicability of Micro-FTIR in Detecting Shale Heterogeneity*

Maria Mastalerz[1], Carley Gasawal[2], Fed Krause[3], Chris Clarkson[3], and Chris DeBuhr[3]

Search and Discovery Article #51360 (2017)**
Posted February 13, 2017

*Adapted from oral presentation given at SEPM-AAPG 2016 Hedberg Research Conference, Santa Fe, New Mexico, October 16-19, 2016

[1]Indiana Geological Survey, Indiana University, Bloomington, IN 47405, USA (mmastale@indiana.edu)
[2]Department of Geological Sciences, Indiana University, Bloomington, IN 47405, USA
[3]Department of Geoscience, University of Calgary, Calgary, AB, T2N 1N4, Canada

Abstract

Samples of Late Devonian/Early Mississippian New Albany Shale from the Illinois Basin, having maturities ranging from early-mature to postmature (vitrinite reflectance 0.55 to 1.41%) and variable organic matter content (TOC 4.3 to 15.8%), were analyzed with micro-FTIR spectroscopy, ImageJ processing software, and scanning electron microscopic x-ray spectroscopy to explore the distribution, connectivity, and chemical composition of organic matter, clay minerals, carbonates, and quartz, and to further test the applicability of micro-FTIR mapping to study shale heterogeneity. Each sample was analyzed in planes parallel and perpendicular to the bedding in order to investigate anisotropy in component distribution, with a possible implication for better understanding anisotropy in porosity and permeability in organic matter-rich shales. Our results show that for low maturity samples organic matter is better connected in the plane parallel to the bedding than in the plane perpendicular to the bedding. Organic matter connectivity decreases with increasing maturity, as a result of kerogen transformation, but increases again in the post mature stage. Clay minerals are very well connected in both planes, whereas carbonates are not abundant and dominantly isolated in most samples, independent of maturity. This study demonstrates that micro-FTIR mapping is a valuable tool to study shale heterogeneity on a micrometer to millimeter scale, and becomes even more powerful in combination with SEM technique that extends observations to a nanometer scale. However, in order to obtain meaningful and comparable results, micro-FTIR mapping requires very careful standardization, precise selection of peak heights/areas, and mapping conditions (such as aperture size, scan numbers, resolution, etc.) well suited for the analyzed samples.

References Cited

Chen, Y., A. Furmann, M. Mastalerz, and A. Schimmelmann, 2014, Quantitative Analysis of Shales by KBR-FTIR and Micro-FTIR: Fuel, v. 116, p. 538-549. http://dx.doi.org/10.1016/j.fuel.2013.08.052 Website accessed February 2017.

Chen, Y., M. Mastalerz, and A. Schimmelmann, 2014, Heterogeneity of Shale Documented by Micro-FTIR and Image Analysis: Journal of Microscopy, v. 256/3, p. 177-189. http://dx.doi.org/10.1111/jmi.12169 Website accessed February 2017.

Gasaway, C., M. Mastalerz, F. Krause, C. Clarkson, and C. DeBuhr, 2017, Applicability of Micro-FTIR in Detecting Shale Heterogeneity: Journal of Microscopy, v. 265/1, p. 60-72. http://dx.doi.org/10.1111/jmi.12463 Website accessed February 2017.

Gasaway, C., M. Mastalerz, F. Krause, C. Clarkson, and C. DeBuhr, in press, Compositional Heterogeneity of the Late Devonian Middle Bakken Member; Insights from Micro-FTIR and SEM Techniques: Bulletin of Canadian Petroleum Geology, submitted 2016.

Griffiths, P.R., and J.A. De Haseth, 2007, Fourier Transform Infrared Spectrometry: John Wiley & Sons, 560 p.

Parikh, S.J., and J. Chorover, 2006, ATR-FTIR Spectroscopy Reveals Bond Formation During Bacterial Adhesion to Iron Oxide: Langmuir, v. 22/20, p. 8492-8500.

INDIANA GEOLOGICAL SURVEY

Applicability of Micro-FTIR in Detecting Shale Heterogeneity

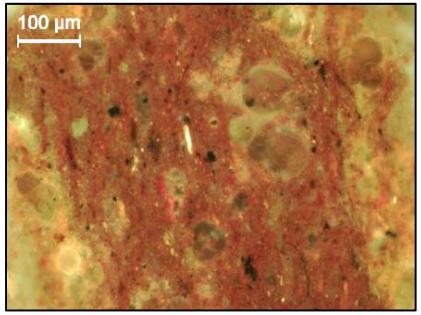

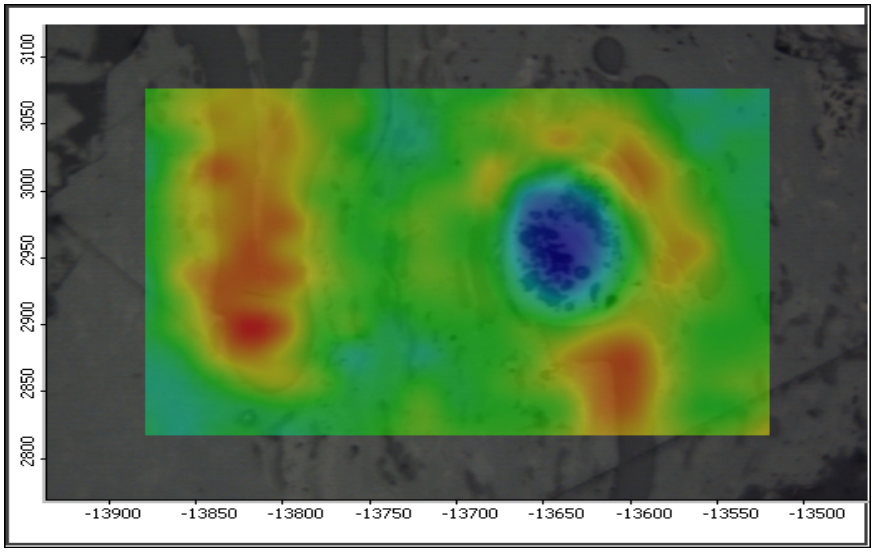

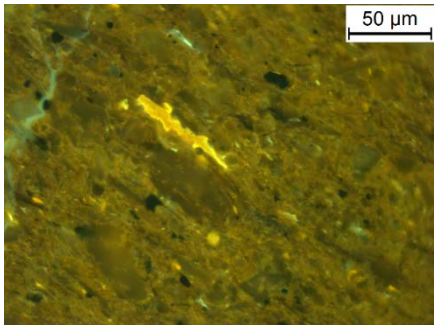

Maria Mastalerz, Indiana University
Carley Gasaway, Indiana University
Fed Krause, Chris Clarkson, Chris DeBuhr, University of Calgary

INDIANA GEOLOGICAL SURVEY

Fourier Transform Infrared Spectroscopy - Functional group distribution

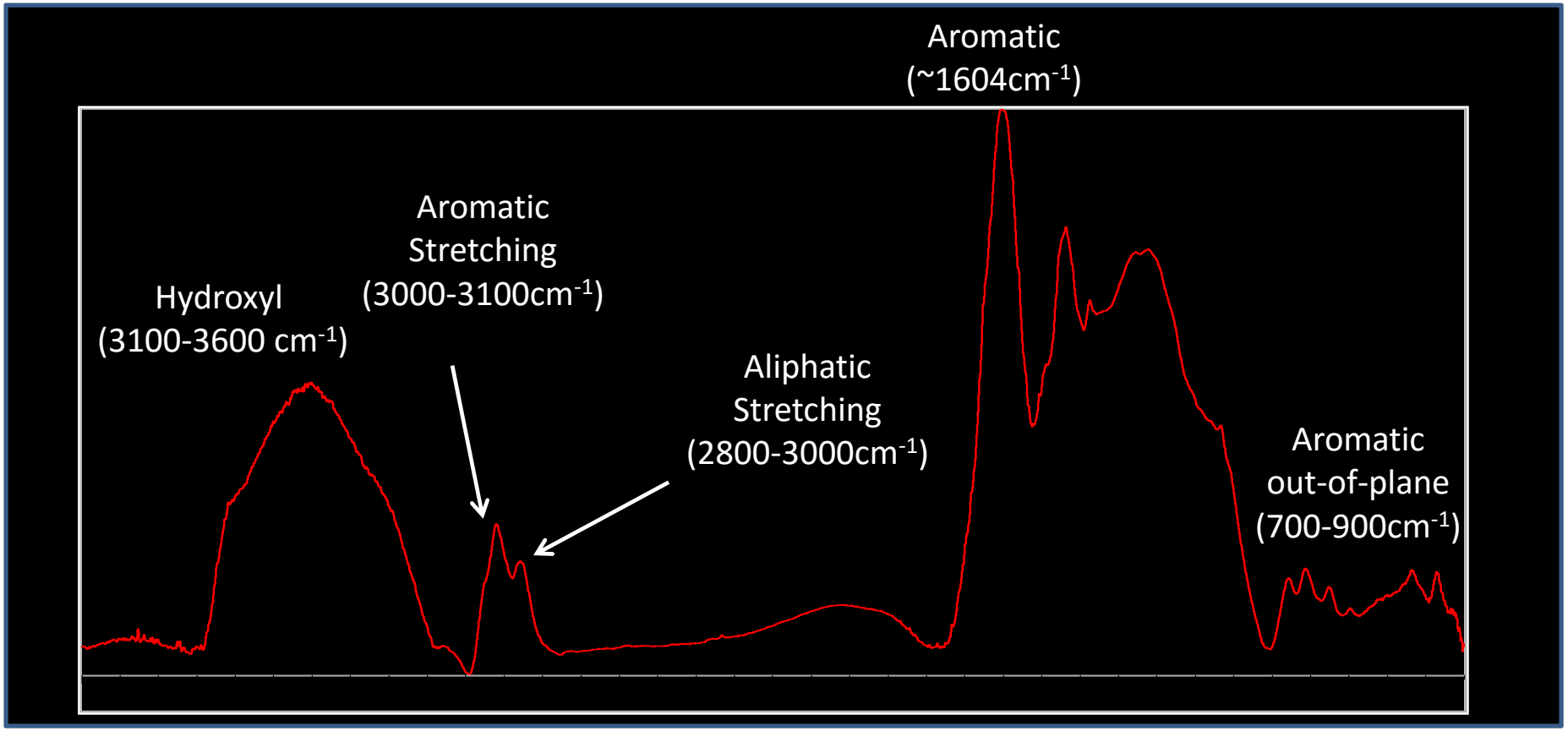

Organic functional groups		Inorganic functional groups	
Wavenumber (cm^{-1})	Assignment	Wavenumber (cm^{-1})	Assignment
3300	OH stretch intermolecular bonding	3698, 3652,1095, 1034,908, 689, 528, 338	Kaolinite
3010	Aromatic C-H	1464, 705, 245	Aragonite
2950	CH_3	1450,882, 729	Dolomite
2920, 2850	Aliphatic CH, CH_2, and CH_3	1431, 869, 307	Calcite
1835	C=O, anhydride	3550, 3400,1615, 1155, 1132,1106 660	Gypsum
1775-1765	C=O, ester with electron withdrawing group attached to single bonded oxygen	1115, 1148, 669	Anhydrite
1735	C=O ester	1075,790, 452	Quartz
1690-1720	C=O, ketone, aldehyde, and -COOH	1052	Smectite
1650-1630	C=O highly conjugated	1015	Oligoclase
1600	Aromatic ring stretch	1006	Glauconite
~1600	High conjugated hydrogen bounded C=O	1001	Muscovite
1560-1590	Carboxyl group in salt from $–COO^-$	984	Chlorite
1490	Aromatic ring stretch	876,727, 713	Ankerite
1450	CH_2 and CH_3 bend, possibility of some aromatic ring modes	407, 396	Marcasite
1375	CH_3 groups	406, 340	pyrite
1300-1100	C-O stretch and O-H bend in phenoxy structures, ethers		
1100-1000	Aliphatic ethers, alcohols		
900-700	Aromatic C-H out-of-plane bending modes		
860	Isolated aromatic H		
833	1,4-substituted aromatic groups		
815	Isolated H and/or 2 neighboring H		
750	1,2-substituted, i.e. 4 neighboring H		

FTIR analysis modes

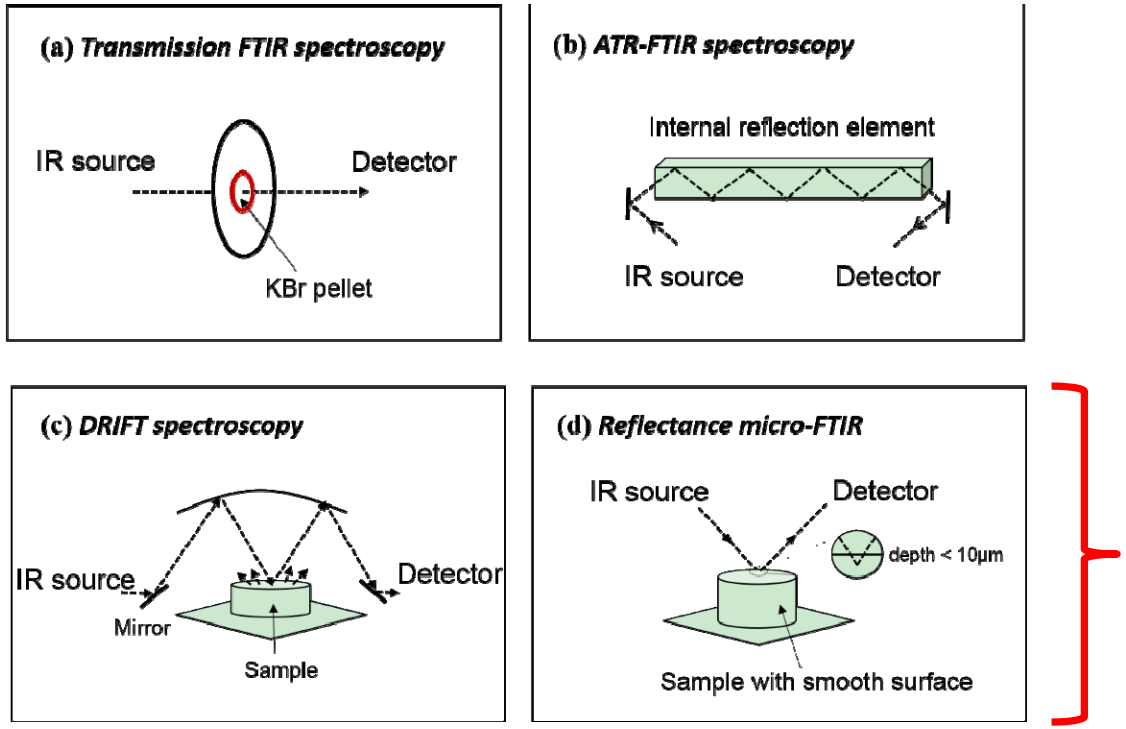

Simplified schematics of common FTIR analysis modes including: (**a**) transmission FTIR; (**b**) attenuated total reflectance (ATR)-FTIR; (**c**) diffuse reflectance infrared Fourier transform spectroscopy (DRIFTS); (**d**) reflectance micro-FTIR. The penetration depth for micro-FTIR is usually less than 10 µm. Modified from Figure 1.3 in Parikh and Chorover [3] and Fig. 15.9 in Griffiths and de Haseth [2].

Micro-FTIR

Fourier Transform Infrared Spectrometer linked with Microscope

Nicolet 6700 FTIR spectrometer

linked with Continuum microscope.

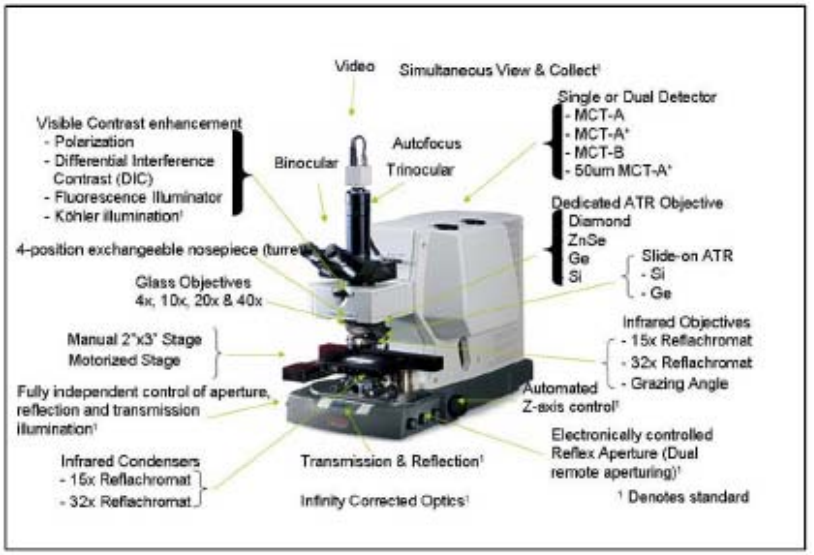

❖An infrared optical system provides the highest available IR spatial resolution and viewing quality

❖Allows analysis of areas as small as 20μm

❖Automatic stage allows mapping of functional groups within a desired are (see next page)

Micro-FTIR spectra of different coal macerals

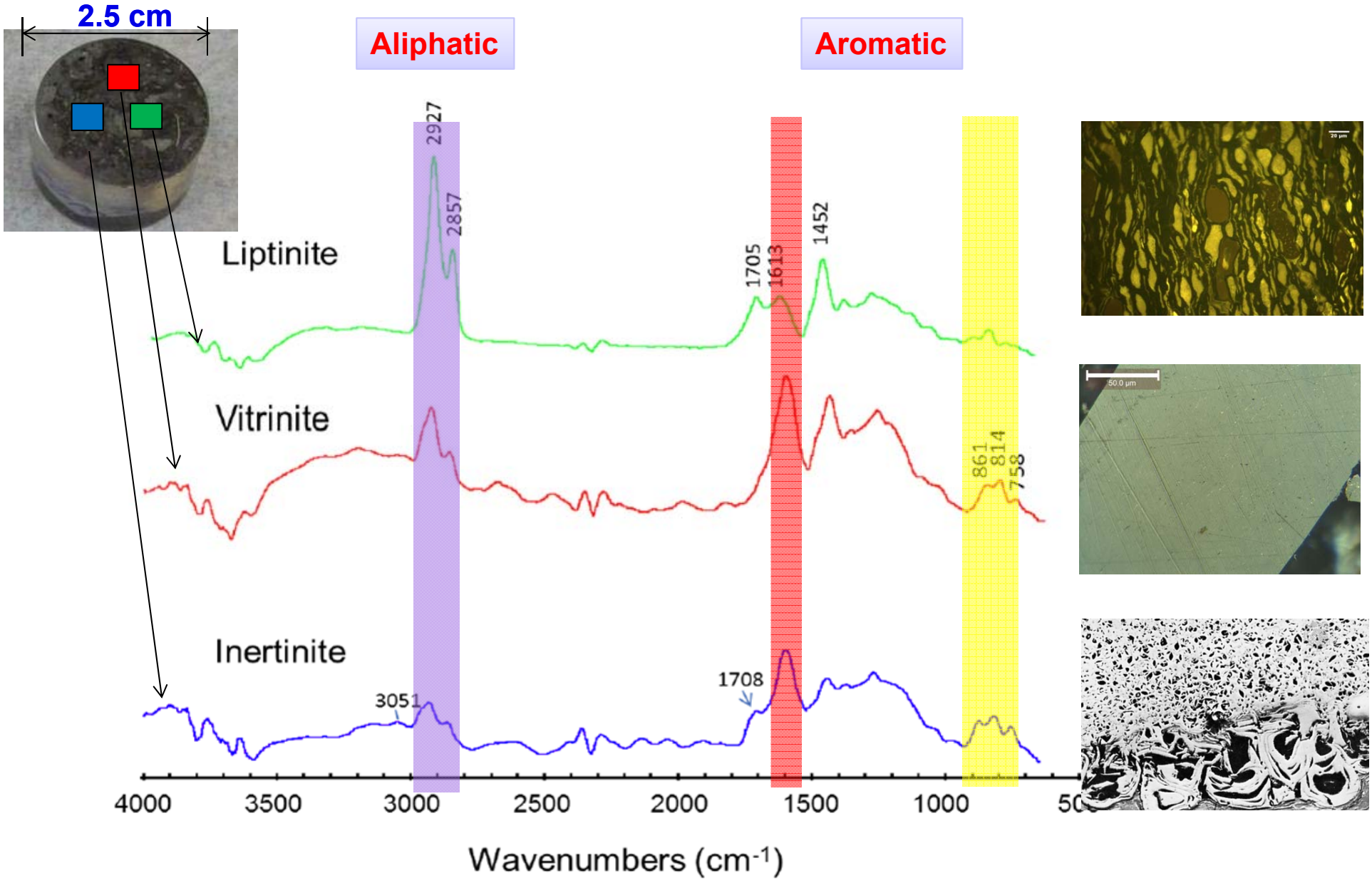

Micro-FTIR mapping

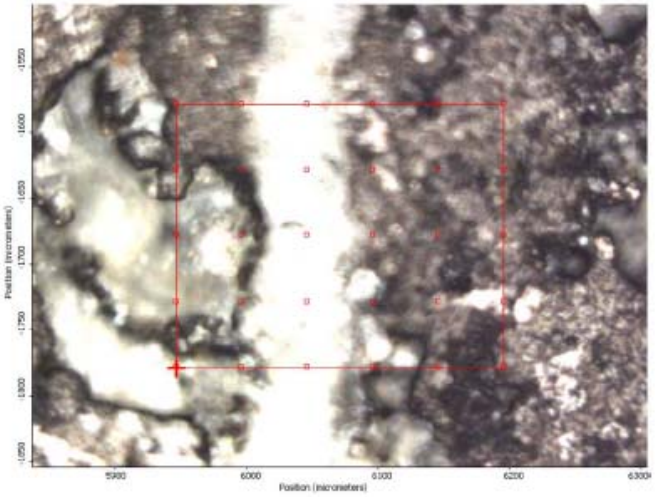

A. Reflected light view of a rock sample with a vein (middle) with mapping area indicated in red. Points for mapping indicated as red spots within the area.

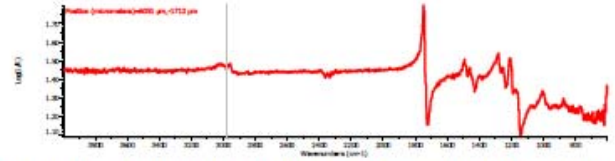

B. Example of a spectrum for one of the spots within the mapping area

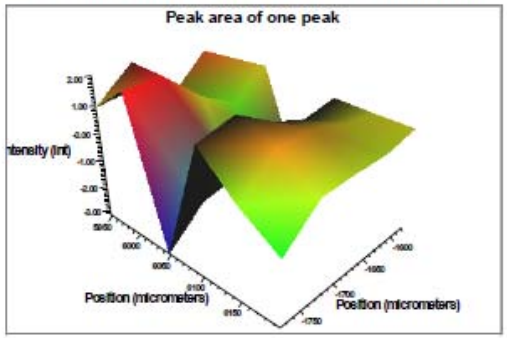

D. 3D image of chemical map C.

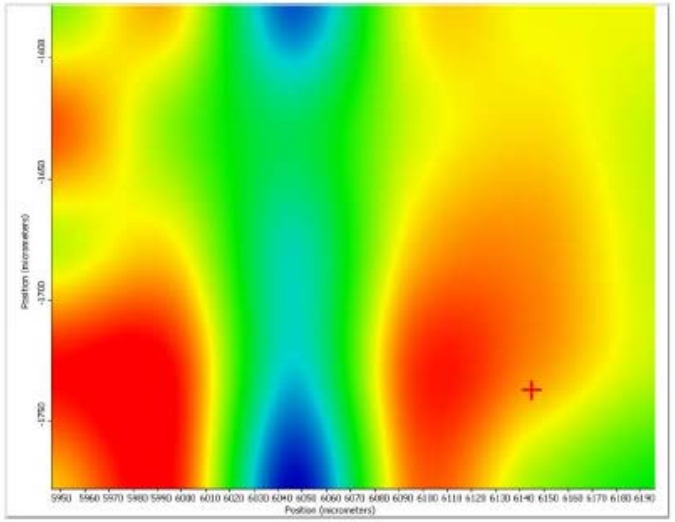

C. Map of the peak area in one spectral region (2800-3000 cm-1)

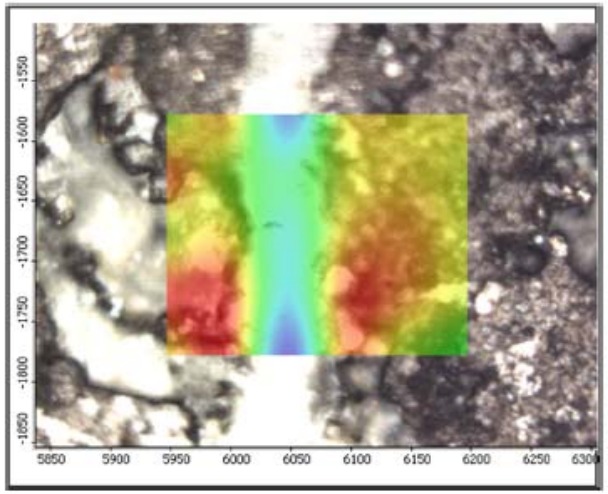

E. Overlap of optical image (A) and chemical map (C)

Micro-FTIR mapping of the chemistry of macerals

Three distinct macerals: sporinite, funginite and vitrinite

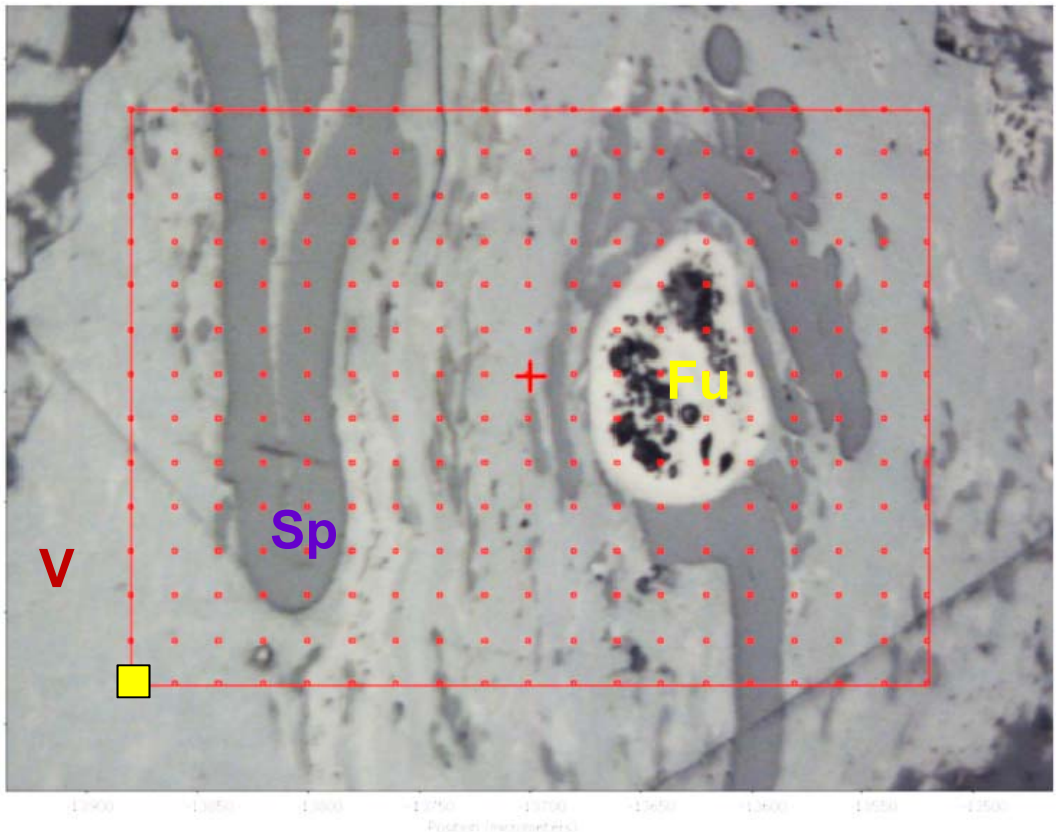

Micro-FTIR microscopic images of the sampling field (R_o = 0.98%)

Point-to-point distance: 20 μm; 266 points in total

Micro-FTIR mapping of the chemistry of macerals

Integrated area of 2800-3000 cm^{-1} absorbance (aliphatic C-H groups)

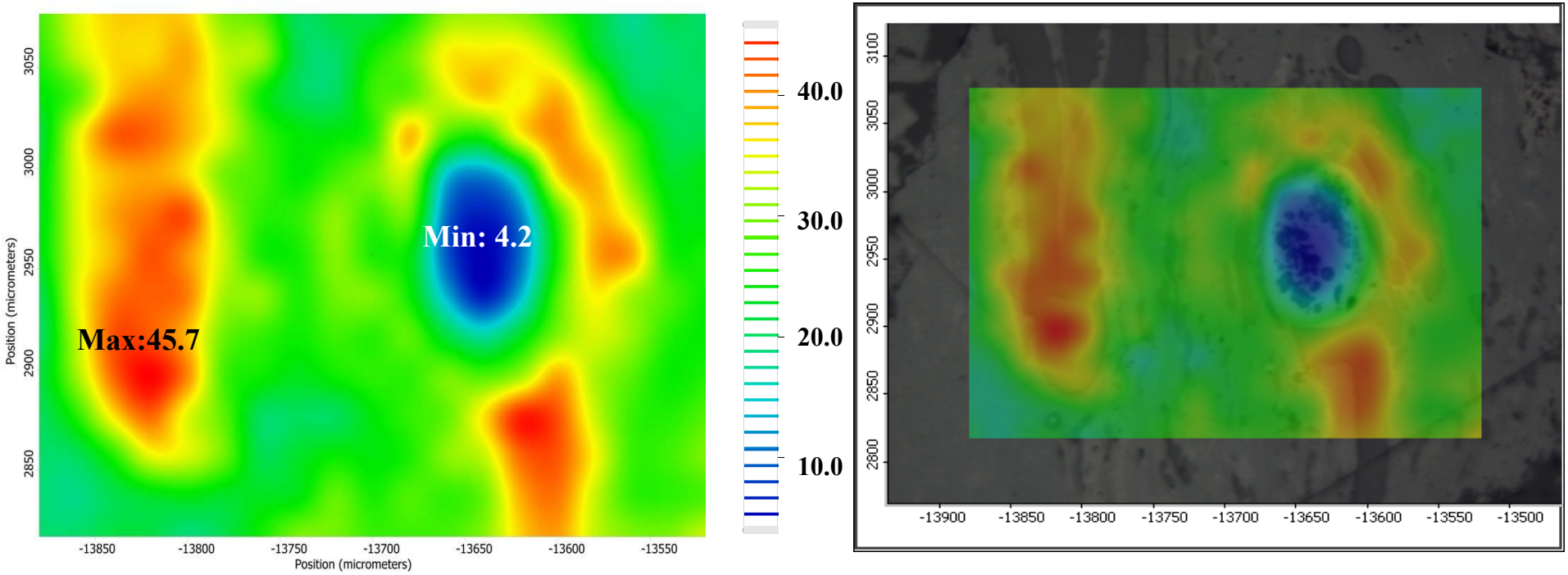

Left: Distribution of aliphatics

Right: Distribution map superimposed on the microscopic video image

Characterization of shales

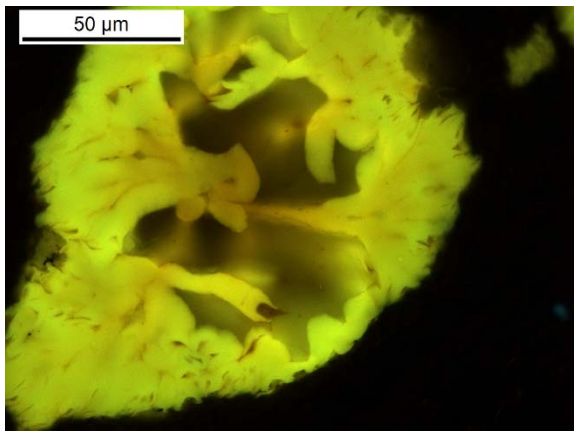

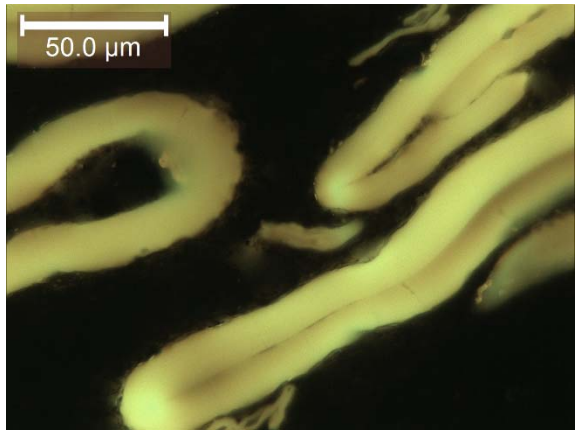

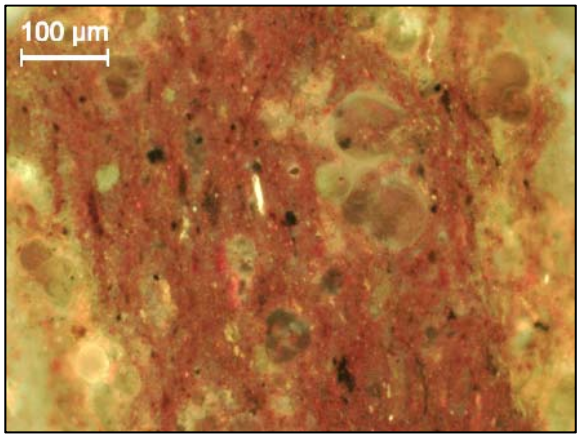

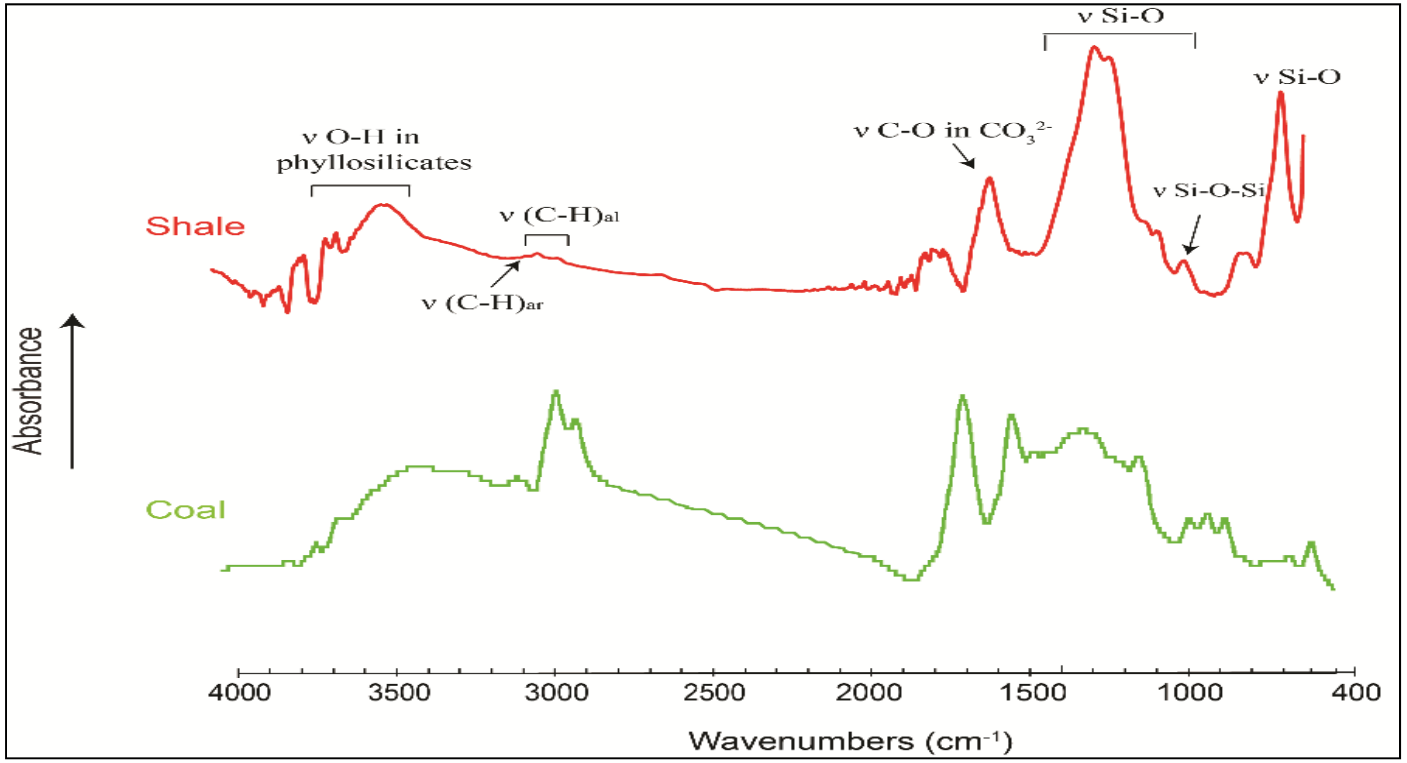

Micro-FTIR spectra of standards

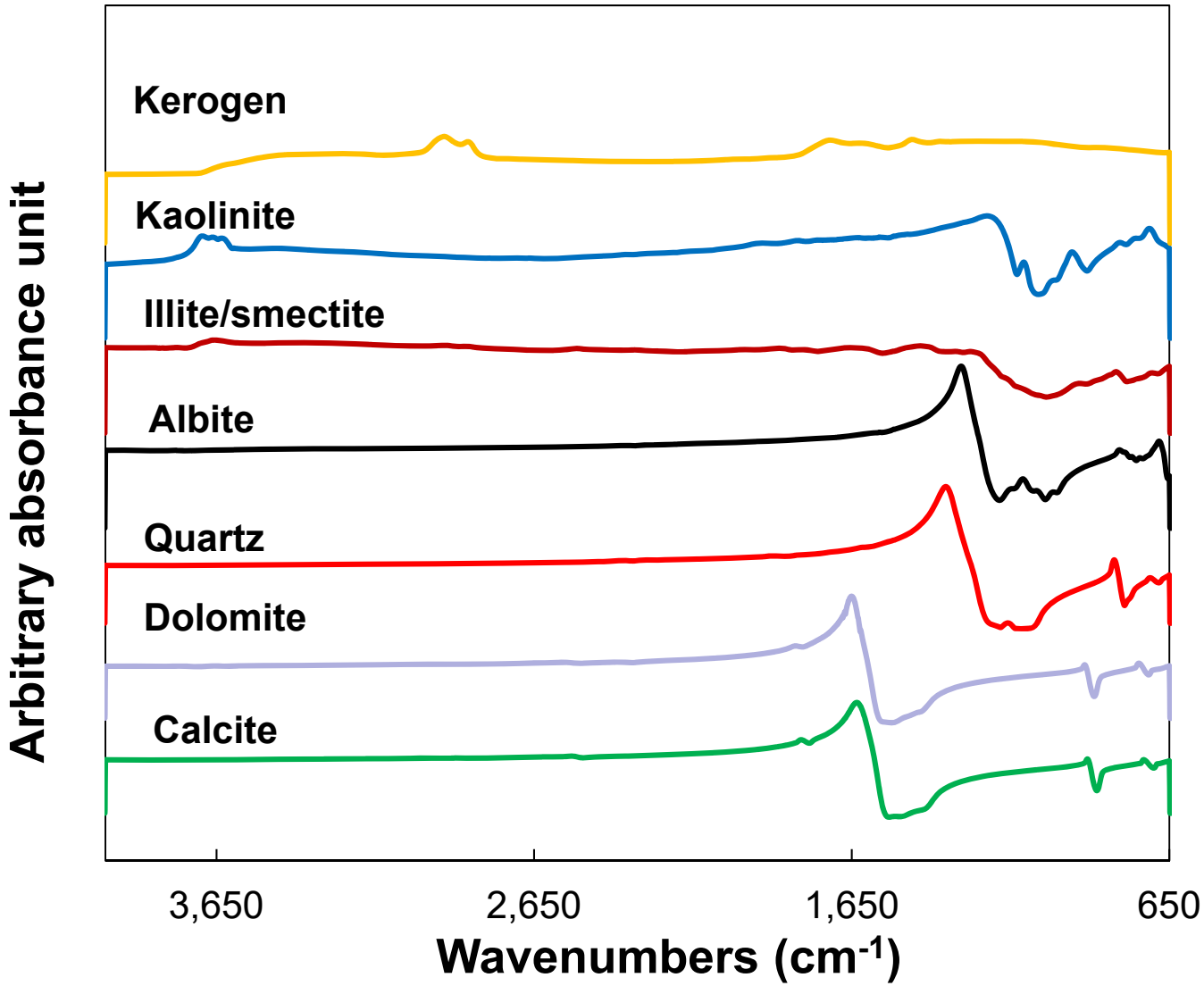

specular reflectance

Reststrahlen bands

Mapping shale heterogeneity – early mature OM rich

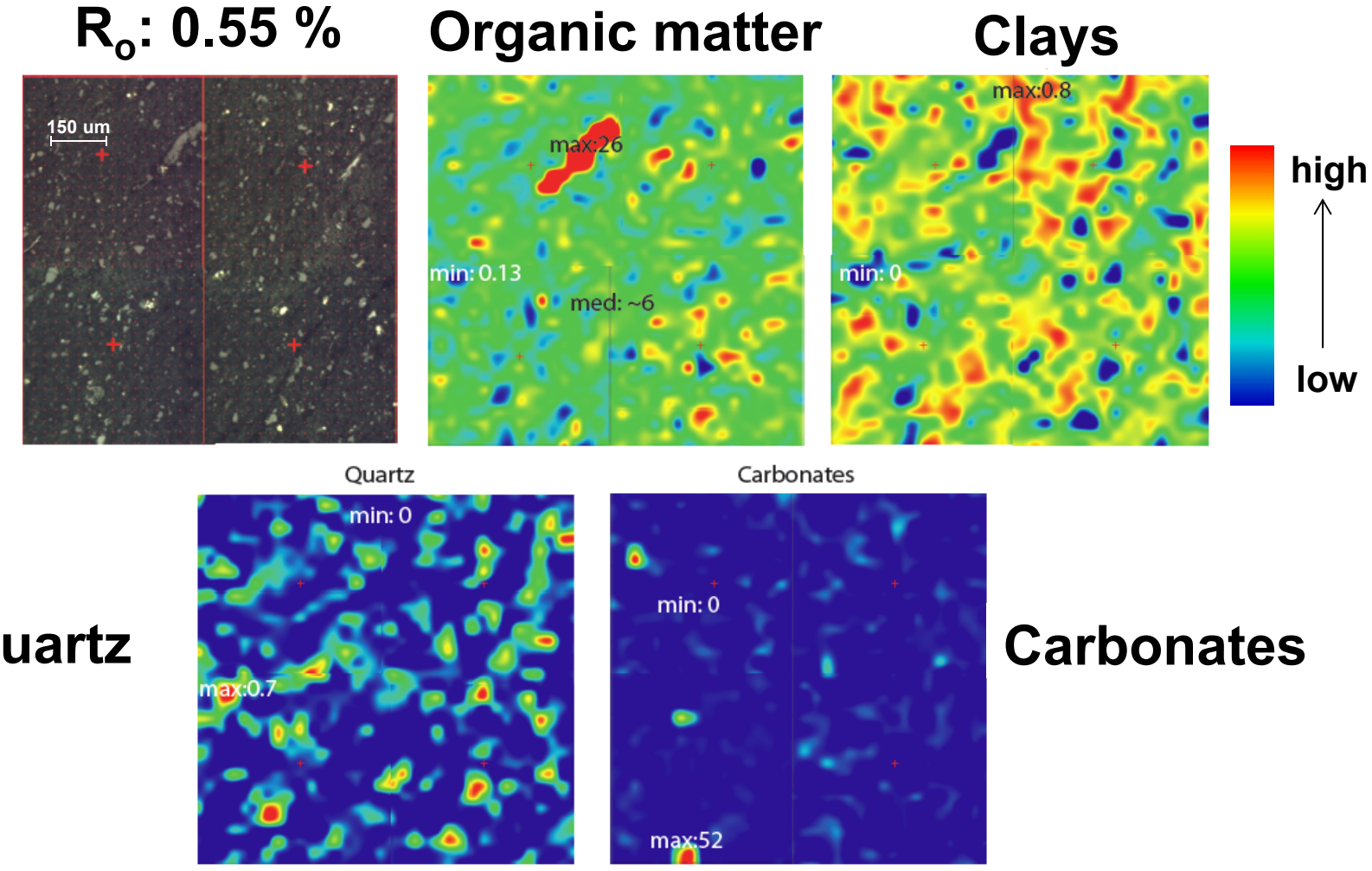

New Albany Shale

TOC: 13 wt. %; Clays: 41 wt. %;
Quartz: 35 wt. %; Carbonates: 1 wt. %

Interconnectivity of organic matter in shale

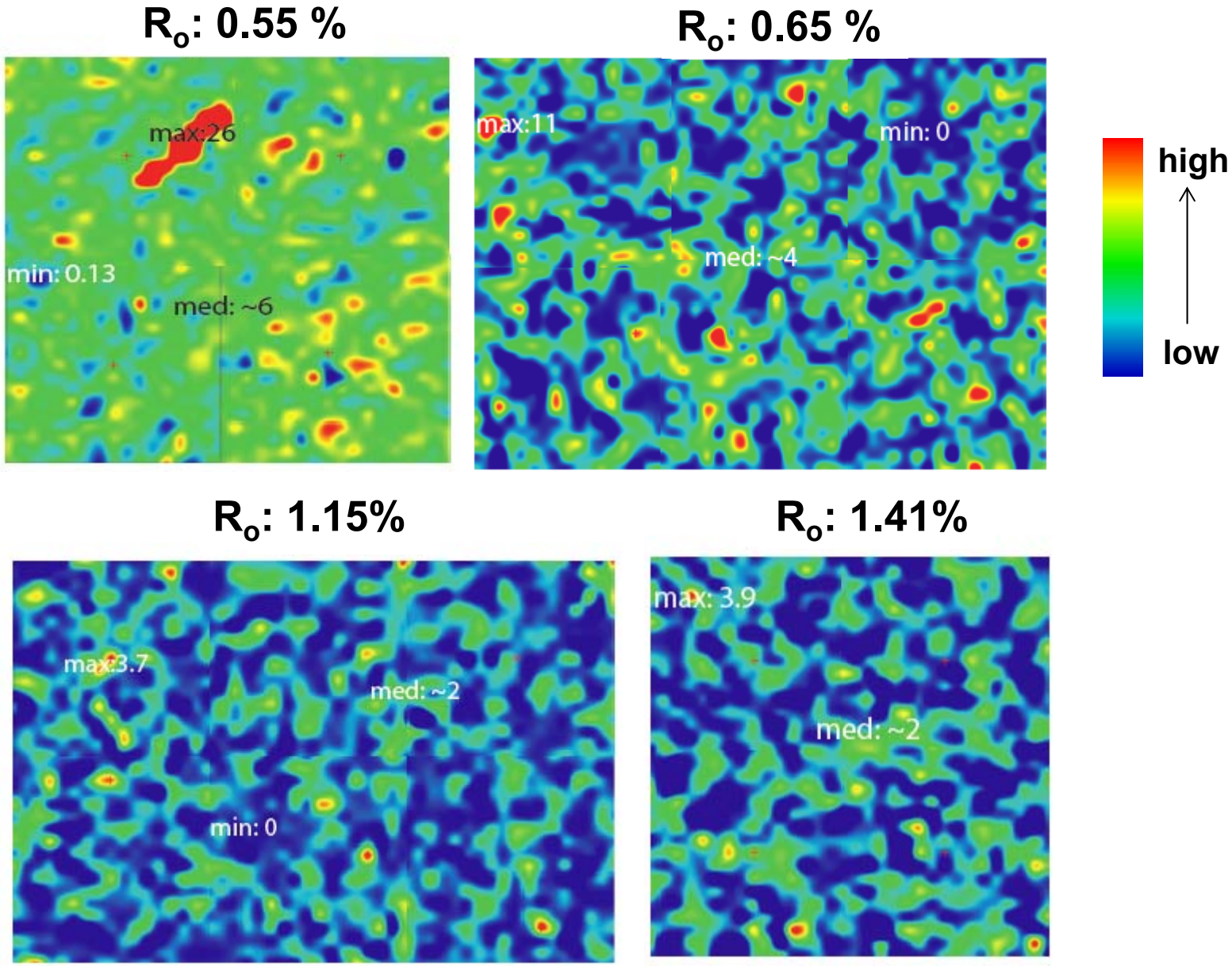

Interconnectivity of organic matter in shale

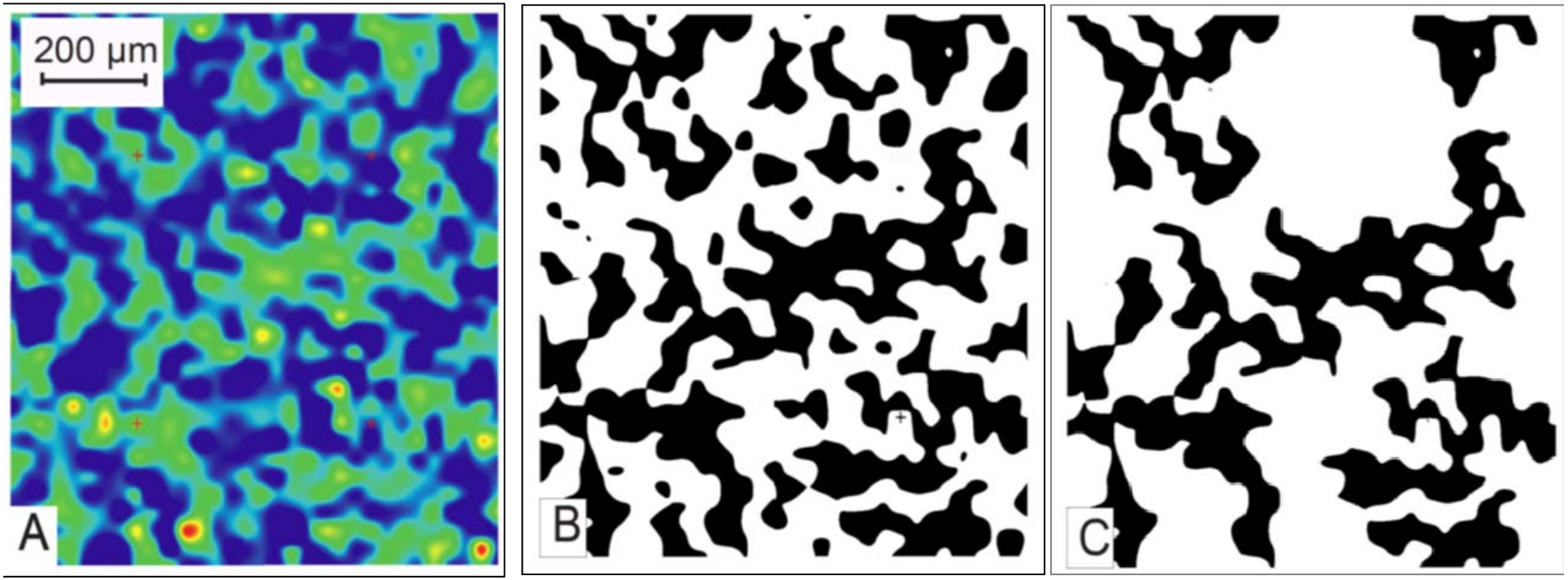

Interconnectivity = [sum of OM domains containing at least one node]/[total OM domains]

Interconnectivity of organic matter in shale

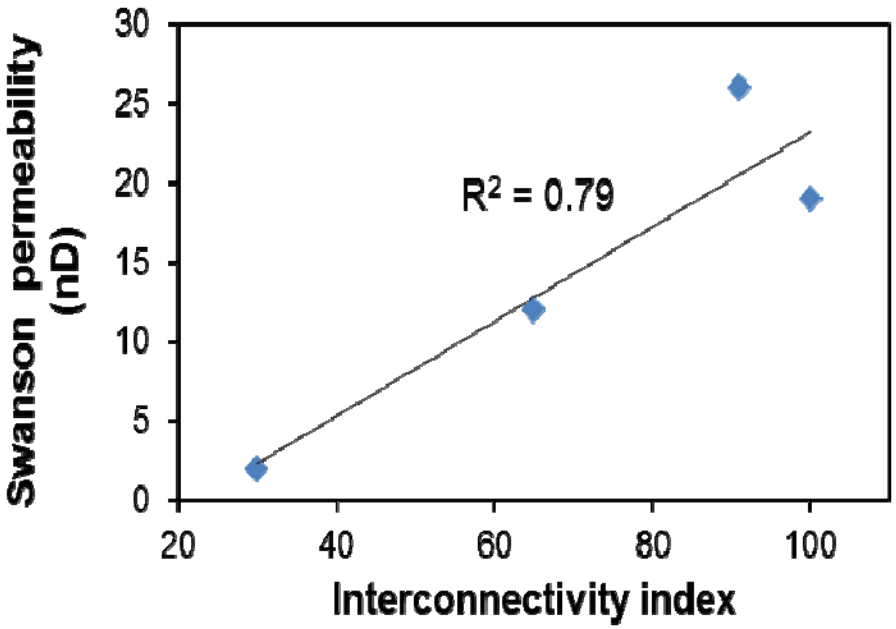

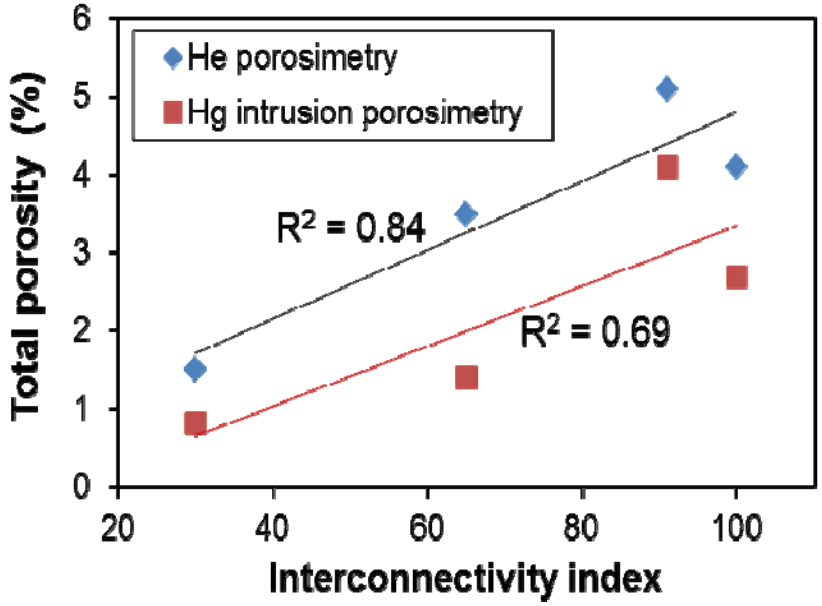

The interconnectivity of OM domains positively correlates with shale permeability and porosity.

Chen, Y., Mastalerz, M., Schimmelmann, A., 2014. Heterogeneity of shale documented by micro-FTIR and image analysis. *Journal of Microscopy* 256, 177-189. http://dx.doi.org/10.1111/jmi.12169

Anisotropy of component distribution

- New Albany Shale
  - Micro-FTIR Mapping (Early Mature)

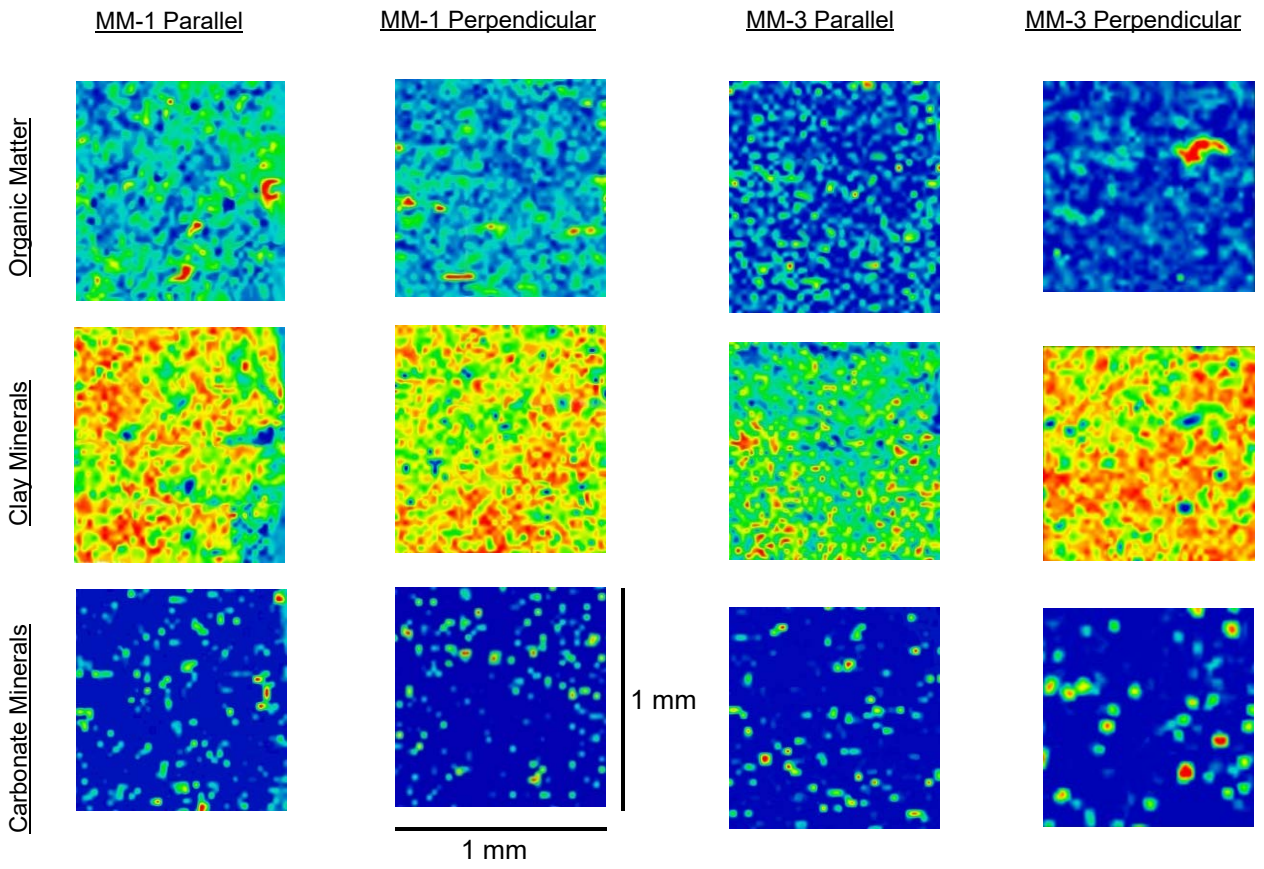

- MM1, with a TOC of 15.8%, shows more organic matter (OM) than MM3, which has a TOC of 5.8%.
- The parallel planes of both samples (visually) seem to have more interconnected OM. This is confirmed by ImageJ processing.
- Clay minerals dominate the shale composition overall, and isolated patches of carbonates exist.

Anisotropy of component distribution

- New Albany Shale
  - Micro-FTIR Mapping (Late Mature)

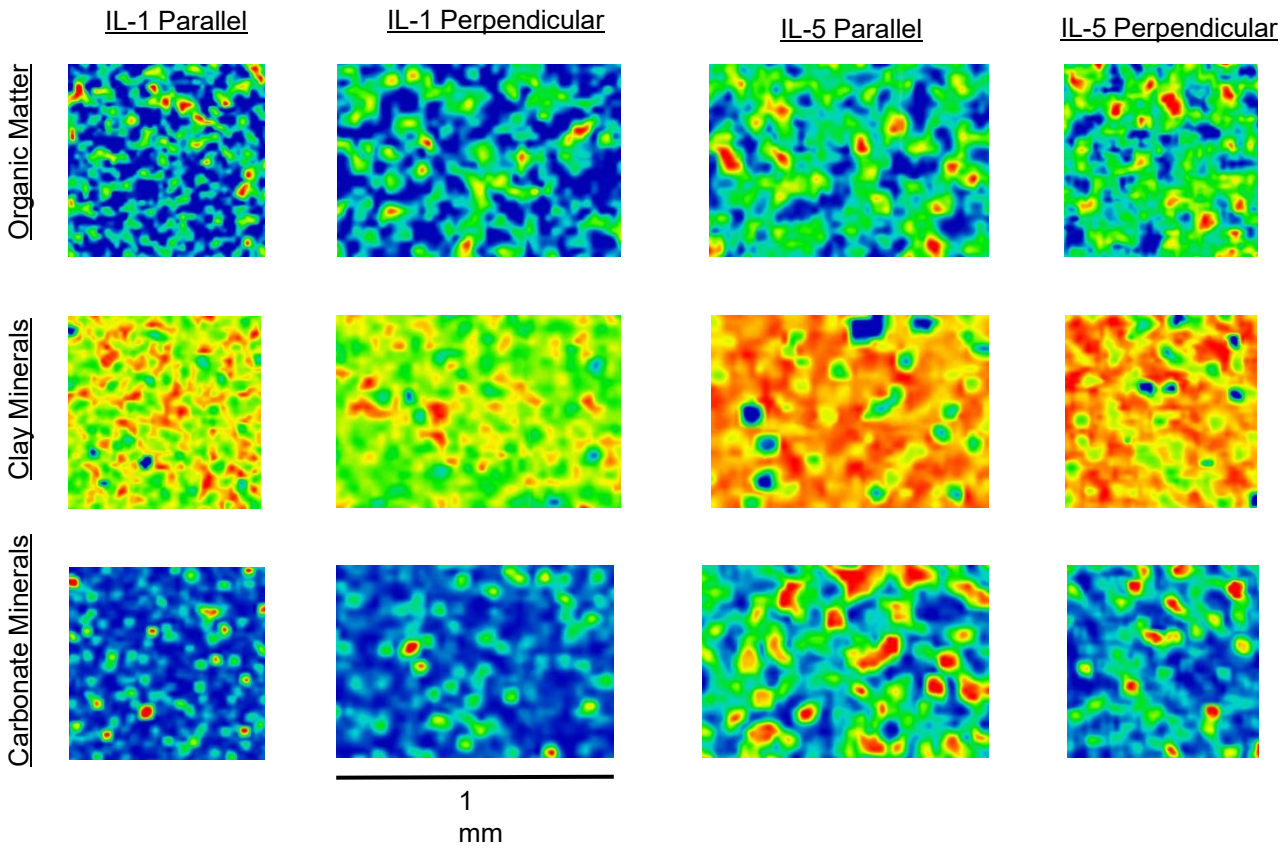

Mapping heterogeneity – early mature OM lean

Mineralogical heterogeneity

Sample	Quartz (%)	Dolomite (%)	Muscovite (%)	Calcite (%)	Feldspar (%)	Pyrite (%)	Anhydrite (%)
BAK 05A	31.7	40.9	9.8	2.3	14.1	1.2	0.1
BAK 07A	41.9	31.7	7.5	1.4	17.0	0.4	0.2
BAK 08A	41.5	33.7	9.1	1.5	13.6	0.6	0.1
BAK 14A	43.1	29.8	9.3	4.0	13.6	0.3	0.1
BAK 24A	41.6	24.4	9.7	8.9	15.1	0.2	0.1
BAK 27A	42.3	27.8	11.3	3.3	15.0	0.3	0.1
BAK 36A	36.3	30.6	8.9	8.2	15.5	0.5	0.1

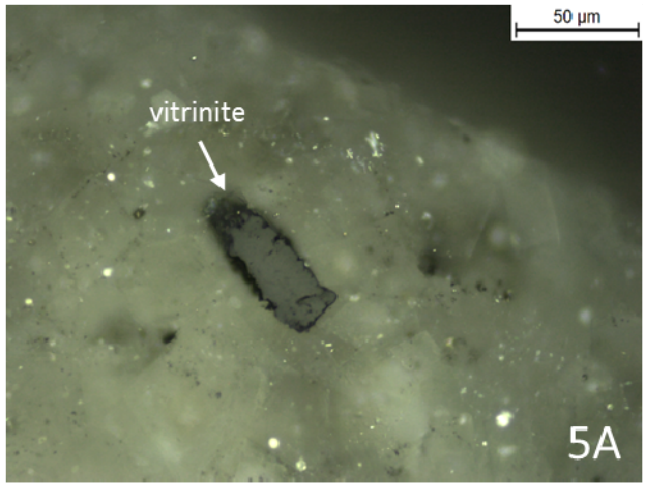

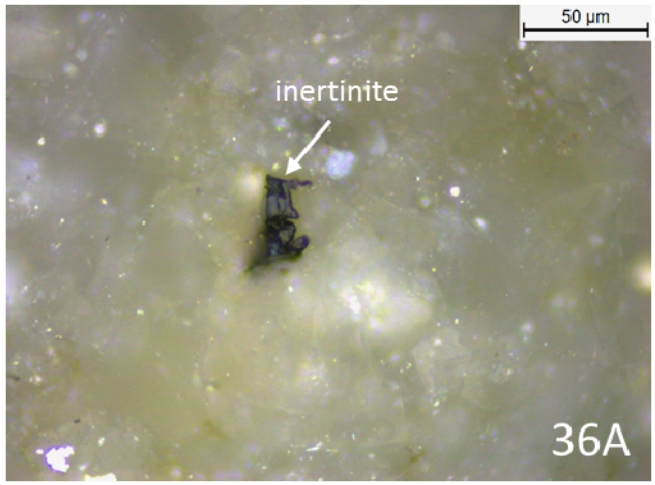

-Dolomitic siltstones
-Organic matter lean
-Vitrinite/inertinite
-Mid mature

Middle Bakken Member

Anisotropy of component distribution

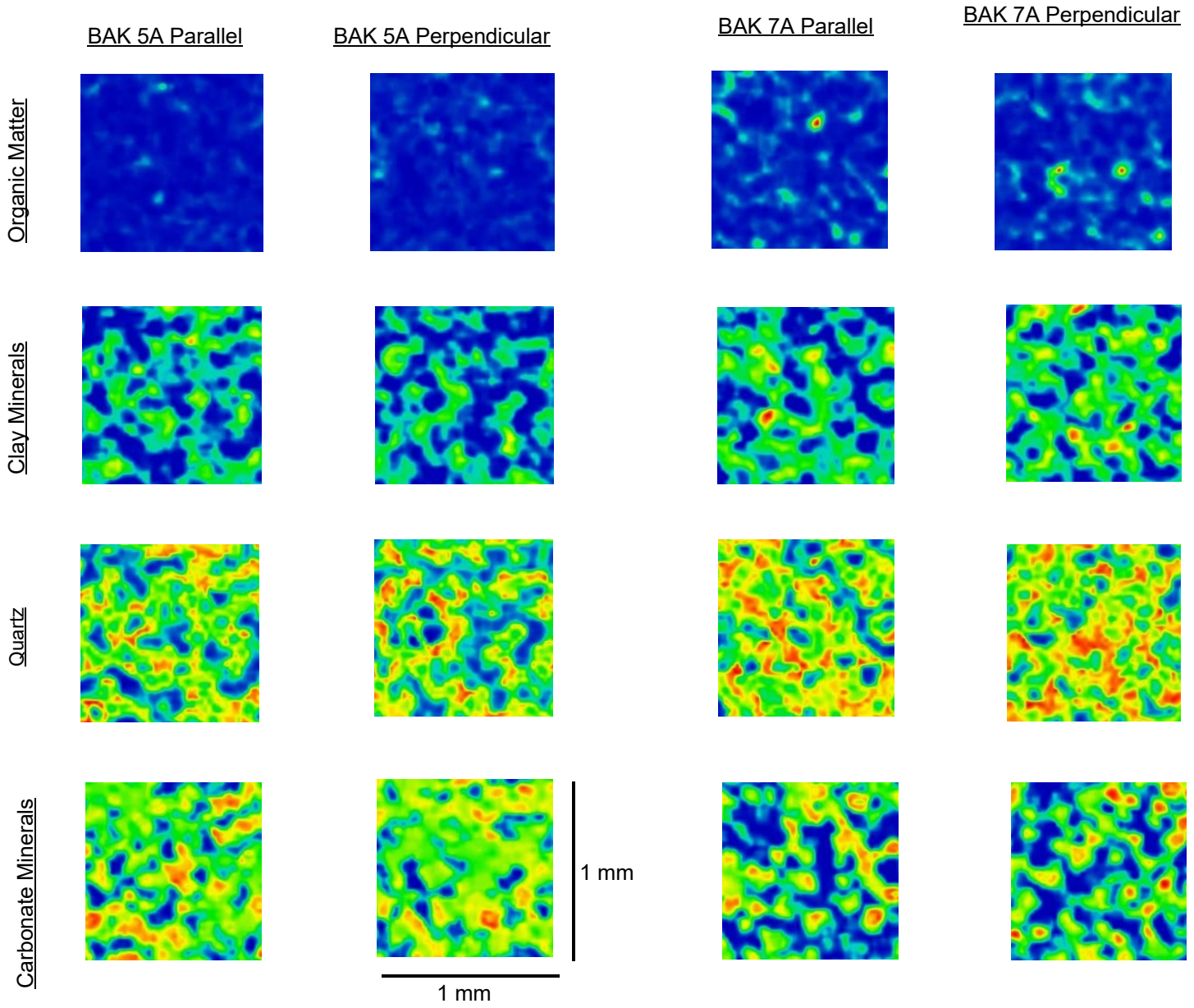

Anisotropy of component distribution

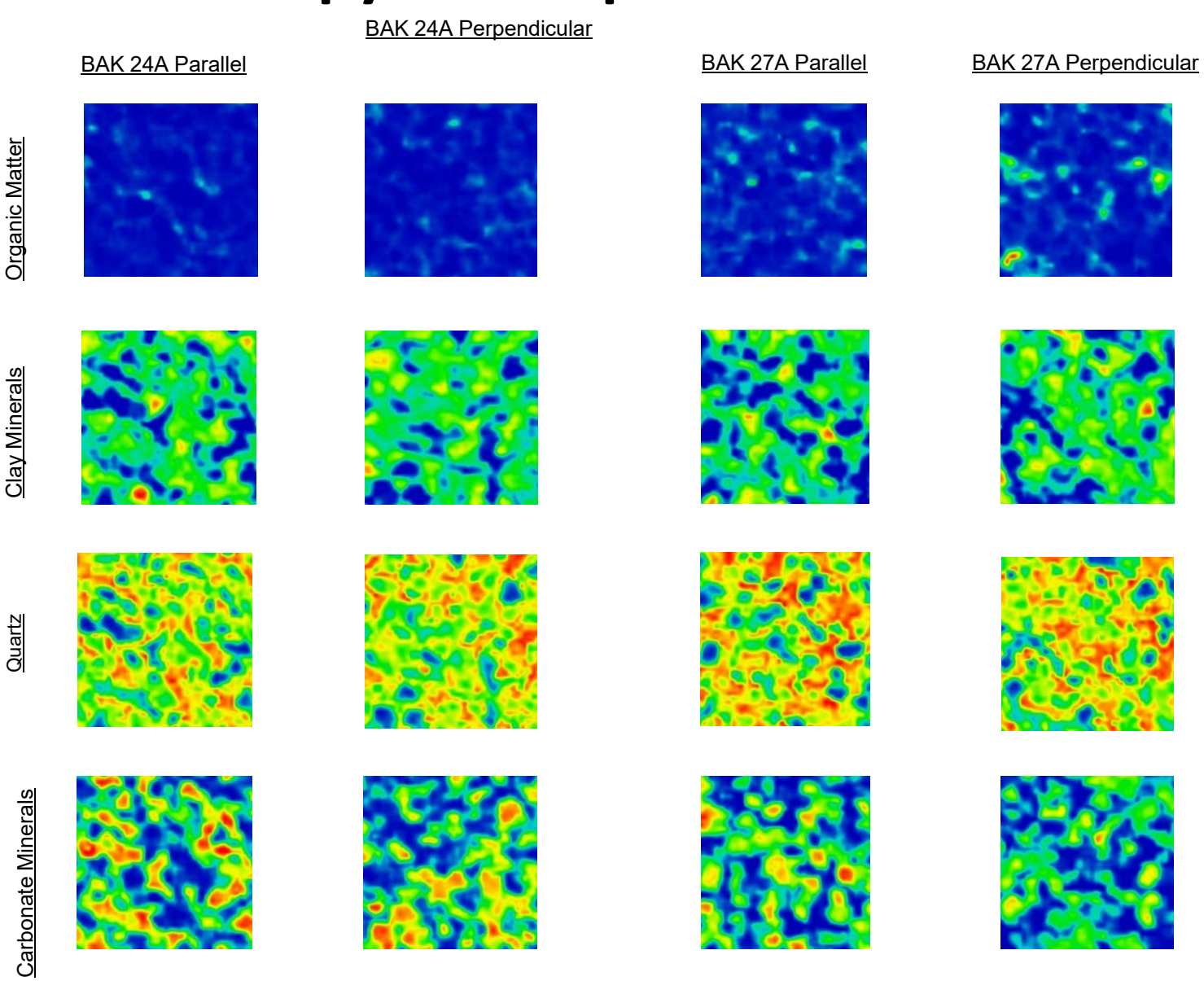

Interconnectivity of organic matter

Sample	Total Area (au)	% of OM in the Total Area	% of Connected OM in the Total Area	% of Isolated OM in the Total Area	I.I.
BAK-5A Parallel	251	0.06%	0.00%	0.06%	0.00
BAK-5A Perpendicular	53	0.01%	0.00%	0.01%	0.00
BAK-7A Parallel	12015	2.56%	0.00%	2.56%	0.00
BAK-7A Perpendicular	13039	2.86%	0.00%	2.86%	0.00
BAK-8A Parallel	5373	1.69%	0.00%	1.69%	0.00
BAK-8A Perpendicular	10781	2.26%	0.00%	2.26%	0.00
BAK-14A Parallel	5293	1.11%	0.00%	1.11%	0.00
BAK-24A Parallel	225	0.05%	0.00%	0.05%	0.00
BAK-24A Perpendicular	249	0.05%	0.00%	0.05%	0.00
BAK-27A Parallel	2443	0.57%	0.00%	0.57%	0.00
BAK-27A Perpendicular	20612	4.36%	0.00%	4.36%	0.00
BAK-36A Parallel	1281	0.27%	0.00%	0.27%	0.00
BAK-36A Perpendicular	14	0.00%	0.00%	0.00%	0.00

Rare and isolated

Interconnectivity of carbonates

Sample	Total Area (au)	% of CARB in the Total Area	% of Connected CARB in the Total Area	% of Isolated CARB in the Total Area	I.I.
BAK-5A Parallel	314219	66.97%	66.97%	0.00%	1.00
BAK-5A Perpendicular	333769	72.40%	72.27%	0.13%	1.00
BAK-7A Parallel	221381	47.74%	44.17%	3.57%	0.93
BAK-7A Perpendicular	229024	49.53%	47.69%	1.84%	0.96
BAK-8A Parallel	136667	44.25%	37.85%	6.40%	0.86
BAK-8A Perpendicular	227965	49.45%	44.19%	5.26%	0.89
BAK-14A Parallel	213540	44.98%	41.59%	3.40%	0.92
BAK-24A Parallel	226732	48.53%	47.33%	1.21%	0.98
BAK-24A Perpendicular	212733	46.42%	42.09%	4.33%	0.91
BAK-27A Parallel	207488	47.07%	44.81%	2.26%	0.95
BAK-27A Perpendicular	196283	41.95%	37.57%	4.38%	0.90
BAK-36A Parallel	334889	69.42%	62.07%	7.36%	0.89
BAK-36A Perpendicular	289952	69.42%	60.81%	8.61%	0.88

Common and well connected

Interconnectivity of quartz

Sample	Total Area (au)	% of Quartz in the Total Area	% of Connected Quartz in the Total Area	% of Isolated Quartz in the Total Area	I.I.
BAK-5A Parallel	290845	61.54%	60.82%	0.71%	0.99
BAK-5A Perpendicular	250724	53.43%	52.67%	0.76%	0.99
BAK-7A Parallel	344264	72.94%	72.72%	0.22%	1.00
BAK-7A Perpendicular	341833	74.37%	74.33%	0.04%	1.00
BAK-8A Parallel	253782	79.11%	79.11%	0.00%	1.00
BAK-8A Perpendicular	348966	73.62%	73.00%	0.61%	0.99
BAK-14A Parallel	368556	78.00%	78.00%	0.00%	1.00
BAK-24A Parallel	351823	75.09%	75.09%	0.00%	1.00
BAK-24A Perpendicular	370000	80.73%	80.71%	0.02%	1.00
BAK-27A Parallel	340863	77.56%	77.55%	0.00%	1.00
BAK-27A Perpendicular	372989	78.34%	77.86%	0.49%	0.99
BAK-36A Parallel	289493	60.56%	60.20%	0.36%	0.99
BAK-36A Perpendicular	332492	71.81%	71.61%	0.19%	1.00

Prominent and well connected

Interconnectivity of clays

Sample	Total Area (au)	% of Clay in the Total Area	% of Connected Clay in the Total Area	% of Isolated Clay in the Total Area	I.I.
BAK-5A Parallel	173940	37.56%	35.80%	1.77%	0.95
BAK-5A Perpendicular	146986	31.46%	26.43%	5.03%	0.84
BAK-7A Parallel	225554	48.85%	44.60%	4.26%	0.91
BAK-7A Perpendicular	268823	58.57%	58.54%	0.03%	1.00
BAK-8A Parallel	189790	60.52%	60.25%	0.27%	1.00
BAK-8A Perpendicular	253445	55.05%	54.68%	0.37%	0.99
BAK-14A Parallel	281310	59.09%	58.92%	0.17%	1.00
BAK-24A Parallel	286262	61.82%	61.82%	0.00%	1.00
BAK-24A Perpendicular	309029	66.73%	66.71%	0.02%	1.00
BAK-27A Parallel	230802	53.24%	52.26%	0.98%	0.98
BAK-27A Perpendicular	272820	59.26%	58.94%	0.32%	0.99
BAK-36A Parallel	170553	35.83%	32.43%	3.39%	0.91
BAK-36A Perpendicular	219421	47.04%	44.49%	2.55%	0.95

Prominent and well connected

Porosity and permeability

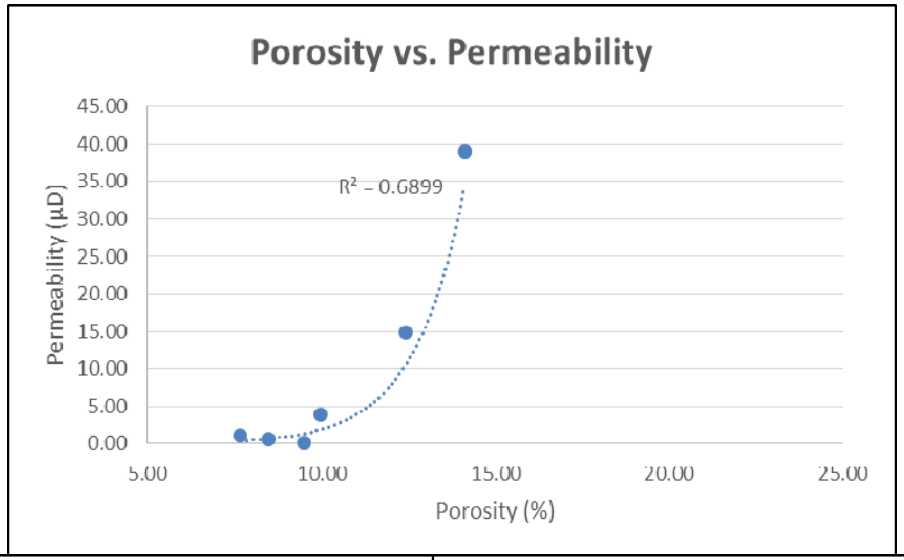

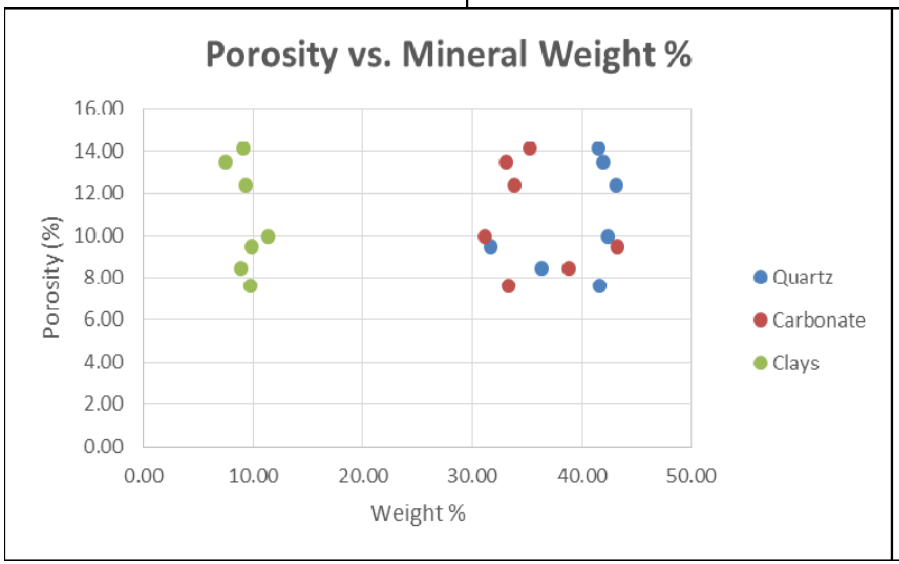

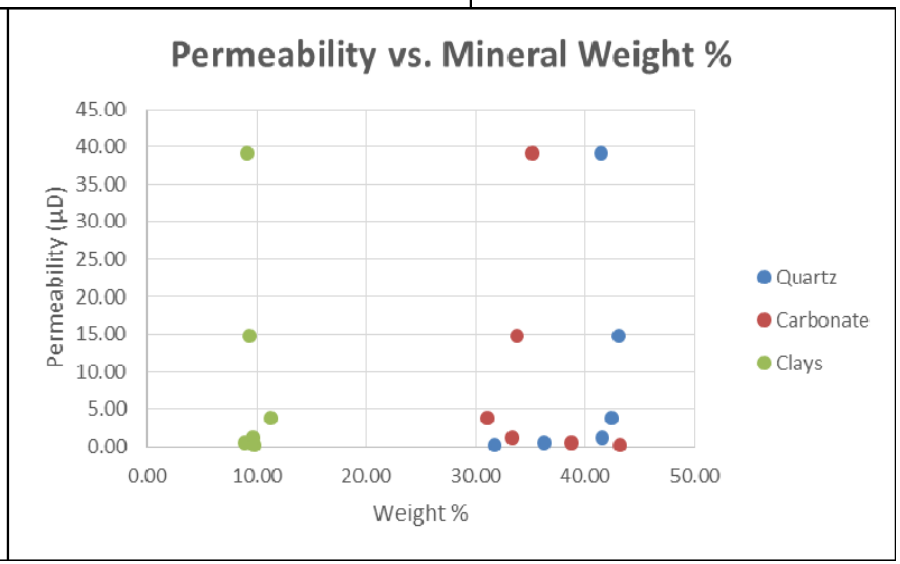

Porosity and permeability

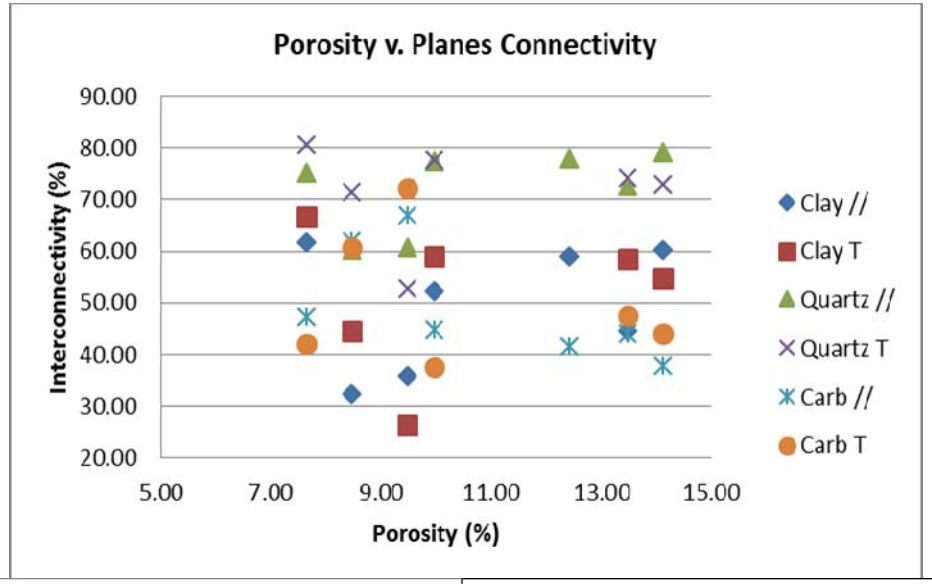

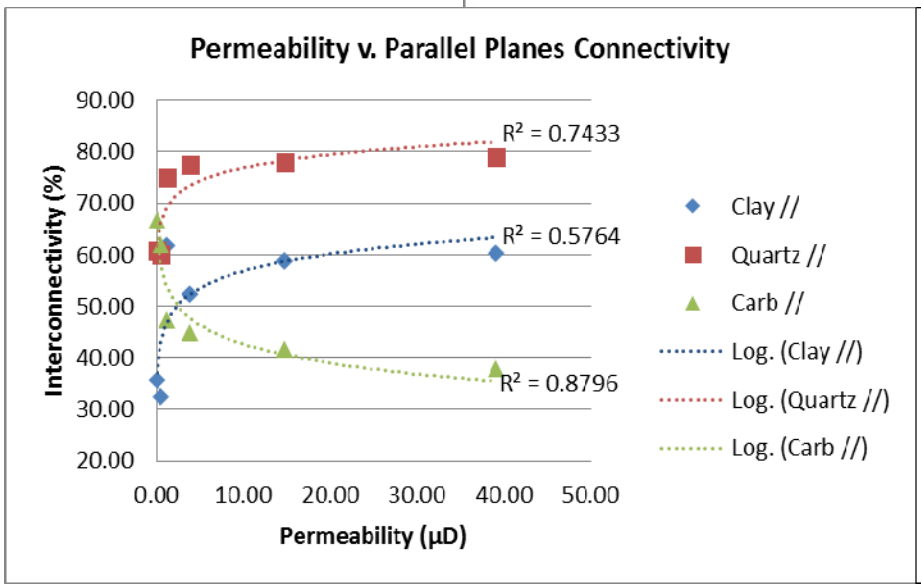

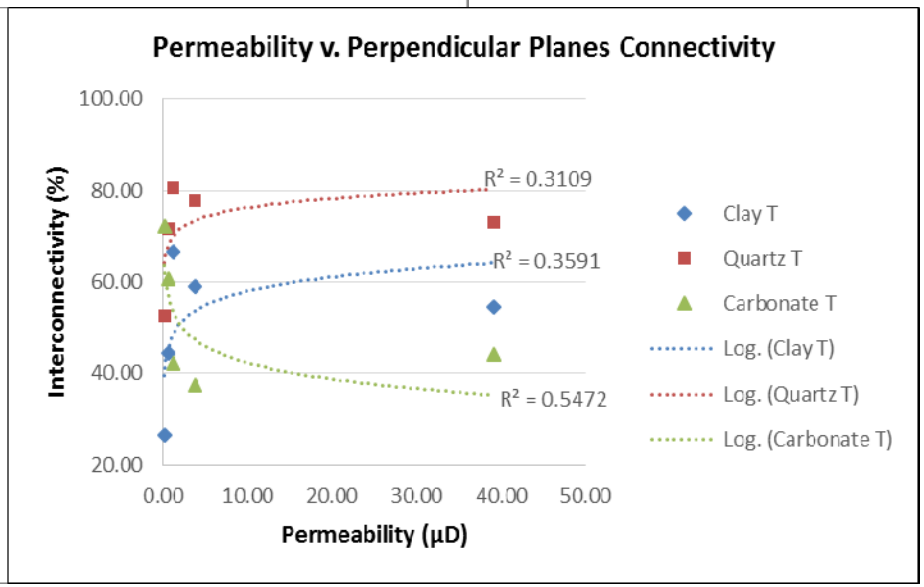

Limitations of micro-FTIR mapping

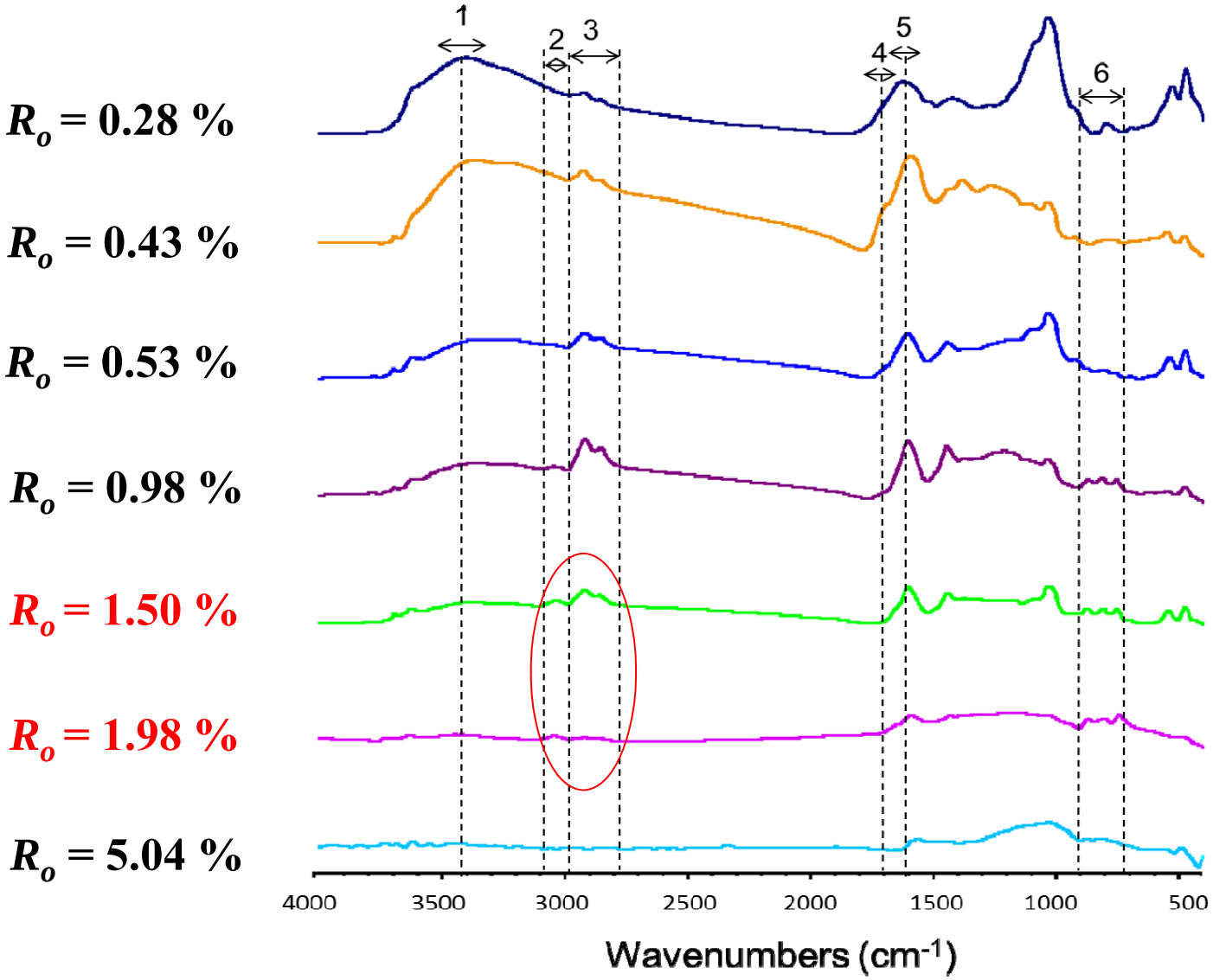

ImageJ mapping of heterogeneity in postmature sample

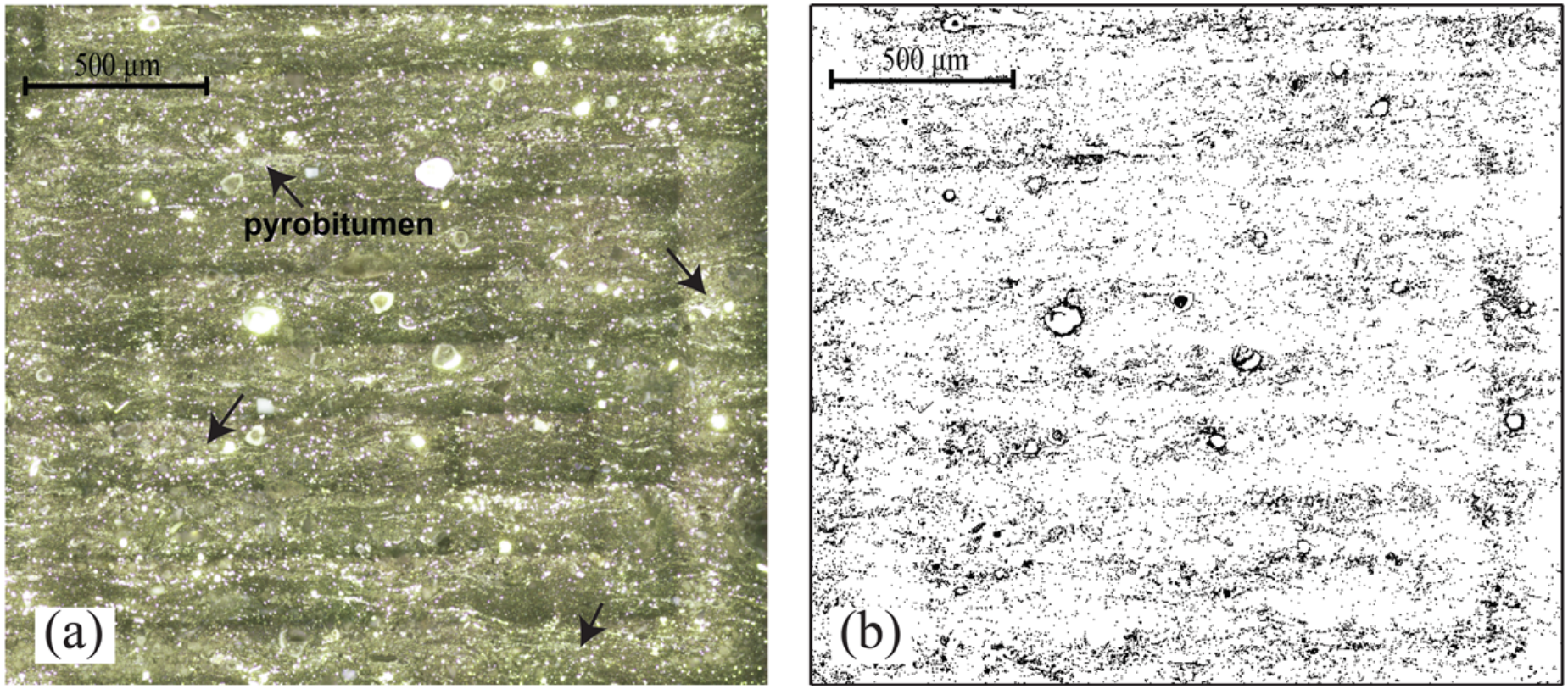

(a) Optical microscopic image across study area. (b) The distribution of pyrobitumen across the same area, analyzed with ImageJ software.

INDIANA GEOLOGICAL SURVEY

CONCLUSIONS

- Micro-FTIR is a powerful technique to analyze heterogeneity of organic-matter rich rocks on a micrometer to millimeter scale. It can map distribution of organic matter, clay minerals, carbonates, and quartz. Clay minerals and carbonates can be mapped, however, only as a group with no resolution into individual minerals possible. Therefore, SEM-XRD, that extends an observation scale to nanometer sizes, is a necessary addition to resolve detailed mineralogical differences.

- In combination with ImageJ processing, micro-FTIR allows us to semi-quantitatively evaluate connectivity of individual components on rock surfaces, which is important information for understanding porosity systems and permeability. Specifically for the organic-matter rich NAS samples studied it shows that in early mature shales there is anisotropy in OM distribution, with OM being better connected in sections parallel to the bedding compared to those perpendicular to the bedding. This anisotropy disappears in late mature stage when OM is already transformed into hydrocarbon products and occurs only in isolated domains regardless of the direction. OM becomes better connected in post-mature stage when abundant pyrobitumen is formed as a result of secondary cracking.

INDIANA GEOLOGICAL SURVEY

CONCLUSIONS

- For OM-lean calcareous mudstones of the Bakken, micro-FTIR shows that distribution and connectivity of quartz, clays, and carbonates all influence permeability. Quartz connectivity has the largest positive influence, followed by clay minerals. In turn, the more connected carbonates become, the less permeable the rock. In contrast to mineral connectivity, the abundance of these minerals does not show a relationship with permeability.
- Correlation between mineral connectivity and permeability and the absence of correlation between mineral connectivity and porosity point to the role of mineral distribution in fluid transport along pathways of high permeability, but not so much in storage in available pores
- Distribution of minerals parallel to the bedding has larger influence on permeability than perpendicular to the bedding, even though their distribution and connectivity was similar in two directions. This further suggests anisotropy in permeability, with higher permeability parallel to bedding.
- Micro-FTIR mapping is still a developing technique and we identified several issues that need to be addressed to get reliable and reproducible results. They include precise standardization, careful selection of peak heights/areas and their verification, and consistency in mapping conditions (aperture, scan numbers, etc).

INDIANA GEOLOGICAL SURVEY

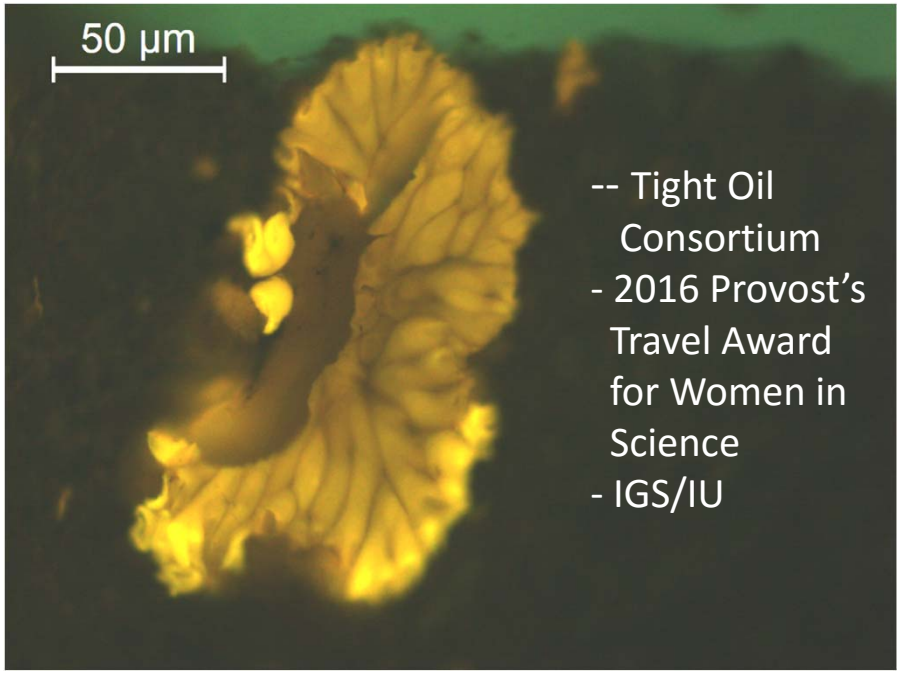

Chen, Y., Furmann, A., Mastalerz, M., Schimmelmann, A. 2014. Quantitative analysis of shales by KBR-FTIR and micro-FTIR. *Fuel* 116, 538-549. http://dx.doi.org/10.1016/j.fuel.2013.08.052

Gasaway, C., Mastalerz, M., Krause, F., Clarkson, C., DeBuhr, C. Applicability of micro-FTIR in detecting shale heterogeneity. Journal of Microscopy, in press 2016. http://dx.doi.org/10.1111/jmi.12463

Gasaway, C., Mastalerz, M., Krause, F., Clarkson, C., DeBuhr, C., Compositional heterogeneity of the Late Devonian Middle Bakken member; Insights from micro-FTIR and SEM techniques. Bulletin of Canadian Petroleum Geology, submitted 2016.